International Journal of Nanomedicine

Dovepress
open access to scientific and medical research

Open Access Full Text Article

ORIGINAL RESEARCH

Biosynthesis of Silver Nanoparticles Using Culture Supernatant of *Shewanella* sp. ARY1 and Their Antibacterial Activity

This article was published in the following Dove Press journal:
International Journal of Nanomedicine

Aftab Hossain Mondal[1,*]
Dhananjay Yadav[2,*]
Sayani Mitra[1]
Kasturi Mukhopadhyay[1]

[1]Antimicrobial Research Laboratory, School of Environmental Sciences, Jawaharlal Nehru University, New Delhi 110067, India; [2]Department of Medical Biotechnology, Yeungnam University, Gyeongsan 712-749, South Korea

*These authors contributed equally to this work

Purpose: In this study, silver nanoparticles (AgNPs) were biosynthesized using culture supernatant of strain *Shewanella* sp. ARY1, characterized and their antibacterial activity was investigated against Gram-negative bacteria *Escherichia coli* and *Klebsiella pneumoniae.*

Methods: The strain *Shewanella* sp. ARY1 was isolated from river Yamuna, Delhi and used for biosynthesis of AgNPs via extracellular approach. Biosynthesized AgNPs were characterized by UV-Visible (UV-Vis) spectrophotometer, fourier transform infrared (FTIR) spectroscopy, X-ray diffraction (XRD), energy dispersive X-ray (EDX), transmission electron microscopy (TEM) and scanning electron microscopy (SEM). Antibacterial activity of AgNPs was determined by well diffusion, broth microdilution and streaking plate assay to determine the zone of inhibition (ZOI), minimum inhibitory concentration (MIC) and minimum bactericidal concentration (MBC), respectively. The effect of AgNPs on treated bacteria was investigated by electron microscopy analysis. Further, the biocompatibility of AgNPs was tested against mice erythrocytes (RBC) by hemolytic assay.

Results: The UV-Vis spectral analysis revealed absorption maxima at 450 nm which confirmed the formation of AgNPs. The FTIR analysis suggested the involvement of various supernatant biomolecules, as reducing and capping agents in the synthesis of AgNPs. The XRD and EDX analysis confirmed the crystalline and metallic nature of AgNPs, respectively. The TEM and SEM analysis showed nanoparticles were spherical with an average size of 38 nm. The biosynthesized AgNPs inhibited the growth and formed a clear zone of inhibition (ZOI) against tested Gram-negative strains. The MIC and MBC were determined as 8-16 µg/mL and 32 µg/mL, respectively. Further, electron microscopy analysis of treated cells showed that AgNPs can damage the outer membrane, release of cytoplasmic contents, and alter the normal morphology of Gram-negative bacteria, leading to cell death. The hemolytic assay indicated that the biosynthesized AgNPs were biocompatible at low dose concentrations.

Conclusion: This study demonstrates an eco-friendly process for extracellular synthesis of AgNPs using *Shewanella* sp. ARY1 and these AgNPs exhibited excellent antibacterial activity, which may be used to combat Gram-negative pathogens.

Keywords: extracellular synthesis, eco-friendly process, AgNPs, antibacterial, Gram-negative bacteria, hemolytic activity

Introduction

Metal nanoparticles (1-100 nm) have gained significant interest in research due to their wide application in various fields of science and technology. Studies have reported several kinds of metal nanoparticles including silver, gold, titanium, zinc, copper, iron, etc., with unique properties compared to their bulk

Correspondence: Kasturi Mukhopadhyay
School of Environmental Sciences, Jawaharlal Nehru University, New Delhi 110067, India
Tel +91 11-26704307
Email kasturim@mail.jnu.ac.in

submit your manuscript | www.dovepress.com
DovePress
http://doi.org/10.2147/IJN.S274535

counterparts.[1–4] Metal nanoparticles have vast application in biomedical and biotechnological fields as antibacterial, antifungal, anticancer, antioxidant, anti-inflammatory, larvicidal, pesticide, drug delivery, tumor detection, biodeterioration, bioremediation, wastewater treatment, etc.[5–8] This has been observed in recent studies, where biosynthesized copper nanoparticles (CuNPs) and silver nanoparticles (AgNPs) were exhibited antibacterial, antifungal, antioxidant, insecticidal and larvicidal activity.[9,10] Moreover, the biosynthesized AgNPs were effective against the biodeterioration of cellulose-based materials, can thus be applied for the conservation of archaeological manuscripts.[11,12] Among them, AgNPs have garnered interest owing to their wide application in biomedical fields including drug delivery, biosensors, gene therapy, diagnostic, catalysis, wound dressings, anti-microbial, anti-inflammatory and anti-cancer, etc.[13–17] The AgNPs also have huge applications in biotechnological fields such as water filtration, food preservation, sanitization, finished fabrics and dressings for injuries, cosmetics, room sprays, clothing, dye removal, nanopesticides, nanoinsecticides, etc.[5,14,18] Moreover, AgNPs are well known for antibacterial activity against a broad range of Gram-positive and Gram-negative bacteria.[15,19,20] Recent studies reported the antibacterial activity of AgNPs against a broad range of clinically significant pathogenic bacterial strains including *Escherichia coli, Klebsiella pneumoniae, Staphylococcus aureus, Bacillus subtilis, Bacillus vallismortis* and *Pseudomonas aeruginosa*.[10,13,17,21–23] The AgNPs have been also reported as potential antibacterial against multidrug-resistant bacteria like *E. coli, S. aureus, Bacillus cereus, Enterobacter hormaechei, K. pneumoniae* and *P. aeruginosa*.[1,19,24,25] The mode of antibacterial activity of AgNPs has been proposed by various authors as its ability to act on multiple target sites including outer LPS, cell wall, cell membrane, proteins and DNA, leading to cell death.[15,20,24,26,27]

Due to the wide application of metal nanoparticles in various fields, the research on the synthesis of various metal nanoparticles has increased significantly during the last decade. Physical and chemical methods are mainly applied for the production of metal nanoparticles, but they are not eco-friendly approaches due to drawbacks like expensiveness, enormous consumption of energy, involvement of hazardous chemicals, and generation of toxic byproducts.[2,28,29] Fortunately, the synthesis of nanoparticles can also be achieved by green biological process which has various advantages like easy, cost-effective, non-toxic, eco-friendly and easy to scale-up, and hence can be an alternative to conventional methods.[5,30] Therefore, the development of such a biological method for nanoparticles synthesis using plants, vitamins, enzymes, and microorganisms (bacteria, algae and fungi) is an emerging research area of nanotechnology.[15,18,22,31,32] Among them, bacteria are mostly preferred for biosynthesis due to their high growth rate, simple handling, and the possibility of genetic engineering.[33] The biosynthesis of metal nanoparticles using bacteria can be achieved by either intra or extracellular processes. Although intracellular synthesis accomplishes better control over the size and shape distribution, the required additional downstream steps in the isolation of nanoparticles make it tedious and costly compared to the extracellular process.[34] Therefore, extracellular synthesis is mostly used for rapid scale-up and easy downstream processing of nanoparticles.[35] Studies have reported the extracellular synthesis of AgNPs using different bacteria such as *E. coli, Pseudoduganella eburnea, Bacillus licheniformis, Bacillus flexus, Pseudomonas* sp., *Shewanella oneidensis, Serratia nematodiphila,* etc.[31,35–40] Among them, the genus *Shewanella* is well known for metal reduction as well as biomineralization and has been reported for biofabrication of various nanoparticles like silver, gold and copper, and might be a better choice for the biogenic synthesis of small monodispersed nanoparticles.[38,41,42]

The increasing prevalence of infectious diseases caused by Gram-negative bacteria creates a serious threat to public health worldwide. Among Gram-negative bacteria, *E. coli* is the most common and is mainly responsible for urinary tract infection, while *K. pneumoniae* leads to pneumonia and bloodstream infection.[43] The fast development of drug-resistance among pathogens increases the morbidity and mortality rates throughout the world and is highly concerning.[44] The World Health Organization (WHO) listed multidrug-resistant *E. coli* and *K. pneumoniae* among the most critical group of bacteria for which new therapies are urgently needed and AgNPs can be used as a potential therapeutic against such pathogens.

Herein, we demonstrated the biosynthesis of AgNPs utilizing strain *Shewanella* sp. ARY1 culture supernatant. Biosynthesized AgNPs were characterized using various techniques including UV-Vis, FTIR, XRD, EDX, TEM, and SEM. Antibacterial efficacy of the biosynthesized AgNPs was evaluated against the Gram-negative pathogens *E. coli* and *K. pneumoniae*. Further, the effect of AgNPs on *K. pneumoniae* was investigated by SEM and TEM analysis. Finally, the hemolytic activity of the

biosynthesized AgNPs was evaluated against mice RBCs to determine their biocompatibility.

Materials and Methods

Materials

Silver nitrate ($AgNO_3$) was purchased from Merck Ltd., India. Bacterial culture media including Luria agar (LA), Mueller-Hinton agar (MHA), Luria broth (LB) and Mueller-Hinton broth (MHB), and standard antibiotics were purchased from Himedia, India. All the glassware and deionized water were sterilized before being used for the experiments.

Gram-negative bacterial strains *E. coli* ATCC 25922 and *K. pneumoniae* ATCC 700603 were used for the antibacterial study. The ATCC strains were gifted by Dr. Benu Dhawan, AIIMS, New Delhi, India.

Isolation and Identification of Bacterial Isolate ARY1

Bacterial isolate ARY1 was isolated from the collected water sample of the Delhi stretch of river Yamuna, India. Briefly, a serially diluted water sample was spread on LA plates and overnight incubated at 37°C. Then, colonies showing different morphology were selected and sub-cultured on the same medium plates for getting a pure isolate. Further, all the obtained isolates were screened for extracellular synthesis of AgNPs, as previously described elsewhere.[35,45] Based on their efficiency in the reduction of $AgNO_3$ to AgNPs, isolate ARY1 was selected and identified by 16S rRNA gene sequence analysis. The obtained 16S rRNA gene sequence was aligned and analyzed using BioEdit program. This sequence was used for similarity search using BLAST in NCBI. The obtained sequence data of strain ARY1 were submitted to GeneBank, NCBI. Further, comparative analyses of 16S rRNA gene sequences obtained in this study and retrieved from NCBI were done using ClustalW in MEGA6 program. The analyzed sequences were used for the construction of phylogenetic tree by MEGA6 program with the neighbor joining method, to represent the phylogenetic position of strain ARY1.

Biosynthesis of AgNPs

The biosynthesis of AgNPs was performed using the method as described previously with slight modifications.-[37,45] In brief, the pure colonies of selected bacterial isolate (ARY1) were inoculated into LB medium (100 mL) and incubated in an automated rotary shaker incubator at 37°C for 24 h at 180 rpm. Then, the supernatant was collected by centrifugation at 8000 rcf for 10 min at 4°C. Finally, 90 mL of supernatant was added into freshly made aqueous $AgNO_3$ solution in a 250 mL reaction vessel and the final volume concentration was adjusted to 1 mM. Culture supernatant alone, 1 mM $AgNO_3$ solution and un-inoculated LB medium with 1 mM $AgNO_3$ solution were taken as controls. All reaction vessels were incubated at 35°C for 6 h for the complete formation of AgNPs. Initially, the synthesis of AgNPs was monitored by visual examination for color change of the reaction mixture. Finally, biosynthesized AgNPs were collected from the solution through centrifugation at high speed (10,000 rpm) for 30 min at 4°C, as described earlier.[46] The obtained AgNPs were dried at 37°C to get the powder form and were used for characterization as well as antibacterial studies.

Characterization of AgNPs

The biosynthesis of AgNPs was confirmed by measuring the absorbance of the colloidal suspension using a UV-Vis spectrophotometer (UV-2450 Spectrophotometer, Shimadzu) at different intervals of reaction times, as described elsewhere.[16] FTIR spectroscopy (Bruker Tensor 37 FTIR) was used in the range between 4000 and 600 cm^{-1} to determine the functional groups of supernatant biomolecules associated with AgNPs.[35,47] The XRD (PANalytical X'PertPro) was performed using Cu-Kα radiation (k=1.54 Å) generated at 45 kV with 40 mA to determine the crystalline nature of powdered AgNPs.[48] The EDX spectrum was performed to analyze the metallic nature of AgNPs using the detector attached with SEM (ZEISS FE-SEM). The shape and size of AgNPs were characterized by TEM (Jeol-JEM 2100, Japan), operating at 200 kV. The AgNPs were dispersed in deionized water and a drop of suspension was placed on carbon-coated copper grids as well as evaporated before being used to take TEM images.[25] The surface morphology of powdered AgNPs was confirmed by SEM analysis (ZEISS FE-SEM). Further, TEM and SEM micrographs were analyzed by Image J software (National Institutes of Health, Bethesda, MD, USA) to determine the size range and average size of nanoparticles.

Antibacterial Activity of AgNPs

Well Diffusion Assay

The well diffusion method was used to determine the antibacterial activity of the biosynthesized AgNPs, as

described earlier with slight modifications.[8,49] In brief, a pure colony of *E. coli* ATCC 25922 and *K. pneumoniae* ATCC 700603 each was grown in MHB medium for overnight at 37°C (180 rpm), and then sub-cultured in the same medium to an adjusted optical density of 0.13 at 600 nm. The prepared inocula were uniformly spread on MHA plates and wells (6 mm) were made in these plates by a sterile cork borer. Then, 20 µL of different concentrations (20, 30 and 40 µg/mL) of AgNPs solution was poured into 3 wells on each culture-loaded MHA plate. At the same time, bacterial culture supernatant and antibiotic cefotaxime (10 µg/mL) was used in 2 separate wells on each plate as controls. All the sample loaded plates were incubated at 37ºC for 18 h. After incubation, the ZOI was measured and recorded in millimeters.

Determination of minimum inhibitory (MIC) and minimum bactericidal concentrations (MBC)

The MIC of biosynthesized AgNPs against test strains was determined by the broth microdilution method using 96-well microtiter plates, as per CLSI guidelines (CLSI, 2018).[50] Briefly, strains were grown overnight in MHB medium at 37ºC with shaking (180 rpm) and then subcultured in the same medium to obtain ~10^6 CFU/mL. The AgNPs solution was two-fold diluted with MHB up to 10 columns and 100 µL of inoculum (~10^6 CFU/mL) was added into to the first 11^{th}columns, and 12^{th}column containing only medium was maintained as control. The culture loaded microtiter plate was incubated at 37°C (180 rpm) for 16–18 h. After incubation, the lowest concentration of AgNPs which completely inhibited the growth of the test strains was considered as MIC. The MBC of AgNPs was determined by streaking the suspension taken from MIC wells and the wells before them with no visible growth on MHA plates and incubating at 37°C for 24 h. After incubation, the minimum concentration of AgNPs showing no bacterial growth on MHA plates was recorded as the MBC.

Tolerance level

Tolerance level of tested bacterial strains against AgNPs was determined using the following formula:[51]

$$\text{Tolerance} = \text{MBC/MIC}$$

The characteristic of the antibacterial activity of AgNPs was determined by the tolerance level indicating the bactericidal or bacteriostatic action against the tested strains. When the ratio of MBC/MIC is ≥16, the antibacterial efficacy of the test agent is considered as bacteriostatic, whereas MBC/MIC ≤4 indicates bactericidal activity.[21]

SEM Analysis of AgNPs-Treated Cells

The morphological change of AgNPs-treated *K. pneumoniae* was observed by SEM analysis using a previously described sample preparation method.[52] Briefly, log-phase cells (~10^8 CFU/mL) were treated with biosynthesized AgNPs at MBC concentration for 4 h at 37°C. At the same time, untreated cells were maintained as control. The cells were washed three times with PB buffer (10 mM sodium phosphate, pH 7.4) and fixed in 2.5% glutaraldehyde for overnight at 4°C. After fixation, the cells were washed with PB buffer and successively dehydrated with ethanol (30% to 100%) for 10 min each. Finally, cells were dried and coated with gold for viewing the images by SEM (EVO 40, Carl Zeiss, Germany).

TEM Analysis of AgNPs-Treated Cells

For TEM analysis of AgNPs-treated cells, we followed a previously described sample preparation protocol.[53] The sample preparation was almost the same as SEM analysis except for the post-fixation of cells with 1% Osmium tetroxide. The cells were dehydrated and fixed in epoxy resin for fine sectioning by a microtome. The section was placed on copper grids and stained with uranyl acetate as well as lead citrate. Finally, dried samples were observed, and images were taken by TEM (Jeol-JEM 2100, Japan).

Hemolytic Activity of AgNPs

The hemolytic activity of biosynthesized AgNPs was determined as described in our earlier publication.[52] In brief, fresh blood was collected from mice and centrifuged (1500 rpm for 10 min). The isolated RBCs were washed 3 times with 35 mM phosphate-buffered saline (PBS, 150 mM NaCl, pH 7.4) and resuspended in the same buffer to 4% (v/v) concentration. The AgNPs were serially two-fold diluted in PBS (100 µL) and added to 100 µL of the RBCs suspension in a 96-well plate. At the same time, 0.1% Triton X-100 treated and untreated RBCs were kept as positive and negative controls, respectively. The plate was incubated at 37°C for 1 h and centrifuged at 1500 rpm for 10 min. Further, 20 µL of supernatant from each well was transferred to 80 µL of PBS in a new microtiter plate. The absorbance of released hemoglobin was recorded by a multimode microplate reader at 414 nm (Molecular Devices, Sunnyvale, CA, USA).

Percentage hemolysis was calculated as:

[(Absorbance of AgNPs-treated sample - Absorbance of PBS)/(Absorbance of positive control - Absorbance of PBS)] × 100

For this experiment, we followed guidelines of CPCSEA (Committee for the Purpose of Control and Supervision of Experiments on Animals) and Institutional Animal Ethics Committee (IAEC-17/2019) JNU, New Delhi, India.

Statistical Analysis

All the results presented in the present study are the means of three independent replicates and standard error was calculated by Prism 8 program (GraphPad Software Inc., La Jolla, CA, USA).

Results

Identification of Bacterial Strain ARY1

Bacterial isolate ARY1 was isolated from the river Yamuna and selected for the biosynthesis of AgNPs based on its efficiency. The analysis of 16S rRNA gene sequence data revealed that strain ARY1 had maximum similarity with *Shewanella* sp. in the NCBI database and was thereafter referred to as *Shewanella* sp. ARY1. The 16S rRNA gene sequence data was submitted in GeneBanK (NCBI) with an accession number MT559806. Also, neighbor joining phylogenetic tree showed cluster with *Shewanella* sp. (Figure 1).

Biosynthesis of AgNPs

In this study, the culture supernatant of *Shewanella* sp. ARY1 was incubated with $AgNO_3$ solution at 35°C for the synthesis of AgNPs. Change in color of reaction mixture during incubation was the primary indication for the formation of AgNPs. The color of reaction mixture turned to light brown after 1 h of incubation, and then the intensity of color steadily increased with reaction time and formed a dark brown solution at 6 h from its initial state (Figure 2). After 6 h of incubation, no significant color change was observed in the reaction mixture, indicating completion of reaction. In contrast, no color change was observed in the control flasks (alone culture supernatant and only 1 mM $AgNO_3$ solution) under the same experimental condition, indicating no formation of AgNPs. However, the appearance of brown color was observed in the control flask containing LB medium with 1 mM $AgNO_3$ solution, indicating the formation of AgNPs (Figure S1).

Characterization of AgNPs

A strong UV-Vis absorbance peak was located at 450 nm after 6 h of reaction which confirmed the synthesis of

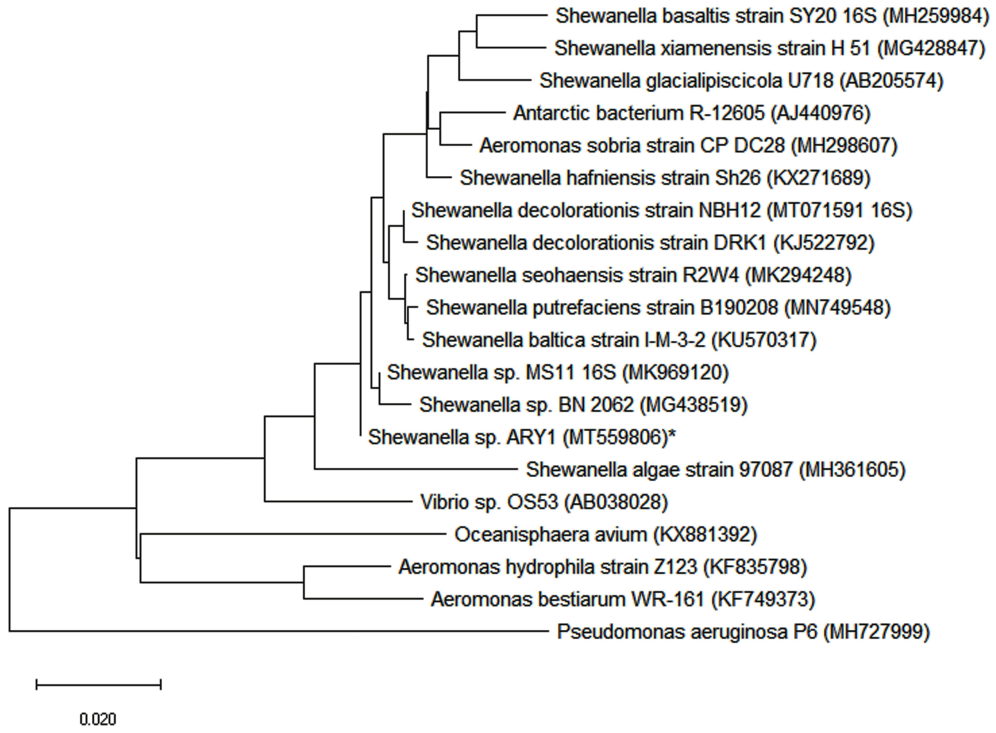

Figure 1 Neighbor joining (NJ) tree showing the phylogenetic relationship of strain ARY1* obtained in this study with related strains of NCBI database using MEGA6 software. The strain ARY1 formed cluster with *Shewanella* sp., scale bar representing 0.020 substitutions per nucleotide position.

AgNPs (Figure 2). The formation of AgNPs increased as the reaction progressed and maximum synthesis occurred at 6 h (Figure 2). The UV-Vis spectral analysis of control suspension (LB with 1 mM $AgNO_3$) showed broadening spectrum with two weak bands at 400 and 515 nm, indicating the synthesis of bigger sizes with different shapes of AgNPs (Figure S1). The FTIR spectrum of AgNPs showed strong absorbance peaks at 3735, 3015, 2250, 1739, 1627, 1527, 1368, 1217 and 1090 cm^{-1} (Figure 3) due to the association of different functional groups of supernatant biomolecules. In the XRD spectrum, four distinct peaks were located at 2θ values of 38.1, 46.18, 64 and 78.08º corresponding to the 111, 200, 220 and 311 Bragg's reflection (Figure 4), confirmed the crystalline nature of AgNPs. The grain size of AgNPs was calculated using Debye–Scherrer's equation:

$D=0.94\ \lambda/\beta\ \cos\theta$, where D is the average crystallite domain size perpendicular to the reflecting planes, λ is the X-ray wavelength, β is the full width at half maximum (FWHM), and θ is the diffraction angle. The grain crystallite size at the most intense 2θ peak was determined as 32.97 nm. Further, EDX analysis was performed to determine the metallic nature of the synthesized nanoparticles, a strong signal was observed at 3 keV, confirming the synthesis of AgNPs (Figure 5). We also observed some other peaks for Cl, C and O in this EDX spectrum. The TEM image of biosynthesized AgNPs showed that the nanoparticles were spherical in shape and their size was in the range of 18.53–72.80 nm, with an average size of 38 nm (Figure 6). Further, SEM image showed spherical nanoparticles with an average size of 39.80 nm (Figure 7), which was in close agreement with the TEM data.

Antibacterial Activity of AgNPs

The antibacterial activity of biosynthesized AgNPs was determined by well diffusion method. A clear ZOI was observed around the wells containing AgNPs against Gram-negative bacteria *E. coli* and *K. pneumoniae* on MHA plates as shown in Figure 8A. The appearance of clear ZOI confirmed the complete growth inhibition of *E.*

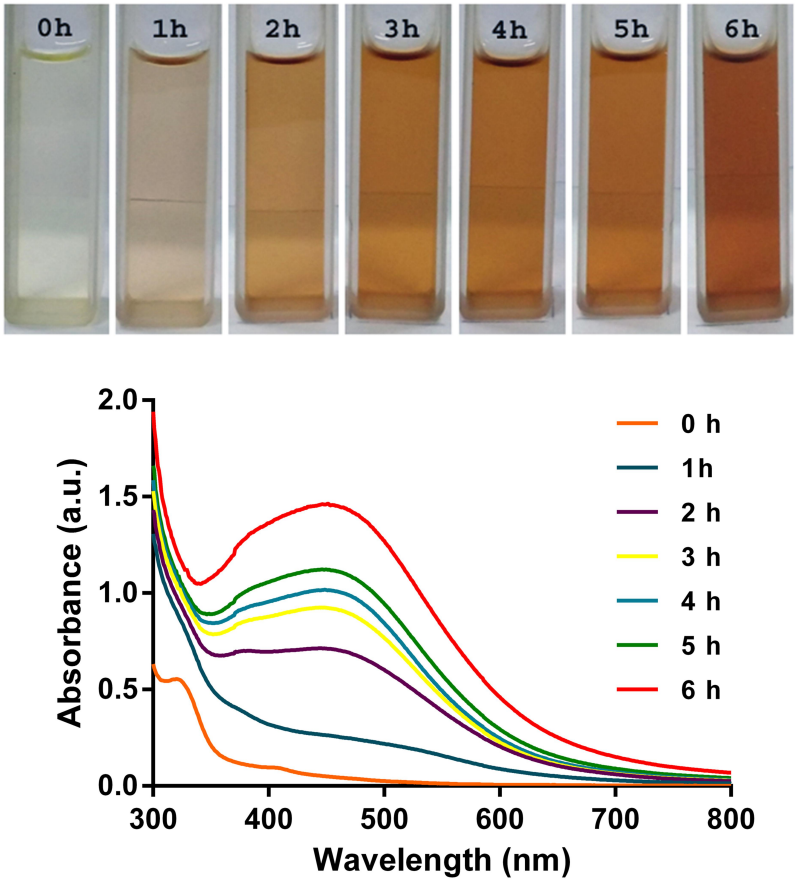

Figure 2 Color changes in the reaction mixture containing *Shewanella* sp. ARY1 culture supernatant along with $AgNO_3$ (top panel) and UV-Vis absorption spectra of biosynthesized AgNPs with the progression of reaction time (bottom panel).

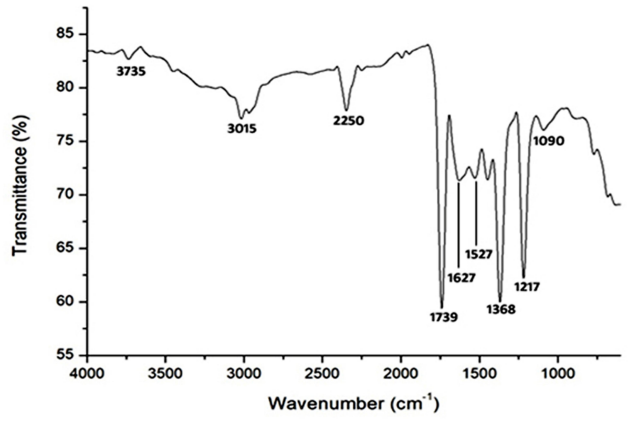

Figure 3 Fourier transform infrared (FTIR) spectrum of biosynthesized AgNPs using culture supernatant of *Shewanella* sp. ARY1.

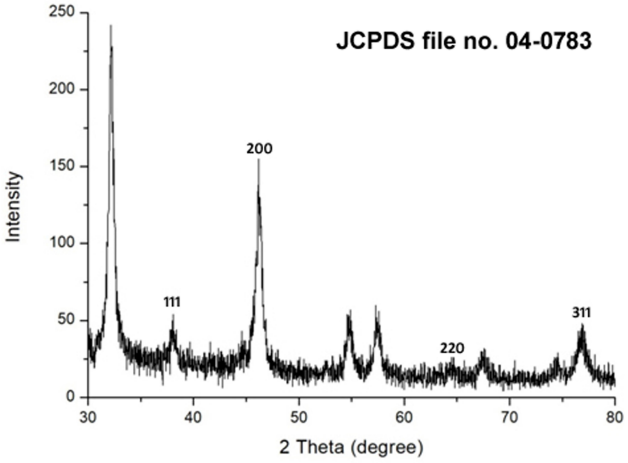

Figure 4 X-ray diffraction (XRD) pattern of biosynthesized AgNPs using culture supernatant of *Shewanella* sp. ARY1.

coli and *K. pneumoniae*. The ZOI diameters of AgNPs and antibiotic cefotaxime were measured in millimeters and represented in Figure 8B. Further, antibacterial activity was evaluated by MIC and MBC assay. MIC was defined as the lowest concentration of AgNPs that inhibits the growth of test strains. The MIC values of AgNPs for *E. coli* and *K. pneumoniae* were 8 and 16 µg/mL, respectively. The MBC, considered as the lowest concentration of AgNPs that killed the test strains resulting in no growth on the LA plates, was determined as 32 µg/mL for both *E. coli* and *K. pneumoniae*. Further, the tolerance level of *E. coli* and *K. pneumoniae* towards AgNPs was determined as 4 and 2, respectively.

SEM Analysis of AgNPs-Treated Cells

The changes in morphology and surface integrity of *K. pneumoniae* cells were observed by SEM, after treatment with the biosynthesized AgNPs at MBC (32 µg/mL) for 4 h, as shown in Figure 9C and D. The SEM images of untreated cells showed normal rod-shaped with intact cell surface (Figure 9A and B). However, the AgNPs treated cells displayed damaged, deformed, and porous outer surfaces with loss of cell wall integrity (Figure 9C and D).

TEM Analysis of AgNPs-Treated Cells

Further, TEM analysis was performed to investigate the ultra-structural changes in the *K. pneumoniae* cells after treatment with AgNPs at MBC (32 µg/mL) for 4 h. TEM images of untreated cells showed an intact cell wall, cell membrane, and homogeneous electron density in the cytoplasm (Figure 10A and B). However, significant changes were observed in the treated cells (Figure 10C and D). The images of treated cells showed lysed cells with damaged outer membrane. The shrinking of protoplasm was also observed due to the leaking out of cytoplasm through a ruptured cell membrane.

Hemolytic Assay

The investigation of hemolytic activity is important to determine the biocompatibility of AgNPs with RBCs in the case of blood contacting AgNPs. Therefore, the hemolytic activity of AgNPs at different concentrations (1–128 µg/mL) was determined against mice RBCs. The percentage of hemolysis was calculated and represented in Figure 11, which depicts that the hemolysis caused by the AgNPs increased with their increasing concentration. The biosynthesized AgNPs showed negligible hemolysis (<1%) till 8 µg/mL and then 6.83±0.75, 18.22±1.2, 34 ±0.11, 46.88±0.54% corresponding to 16, 32, 64, 128 µg/mL, respectively. We used 0.1% Triton X-100, a non-ionic surfactant, as the positive control (100% hemolysis).

Discussion

The increasing prevalence of multidrug-resistant Gram-negative bacteria has compelled the scientific community to develop new alternative therapy to combat them. Silver has been extensively used since ancient times to prevent infection and silver ions also have antibacterial activity. However, both have some drawback like the effect of Ag^+ ions remains for a short time and bacteria are developing resistance against silver due to the occurrence of metal resistant genes.[54,55] These disadvantages of metal can be overcome by the application of AgNPs which have multiple target sites in bacteria such as LPS, cell wall, cell membrane, proteins, and DNA. Hence, it's challenging

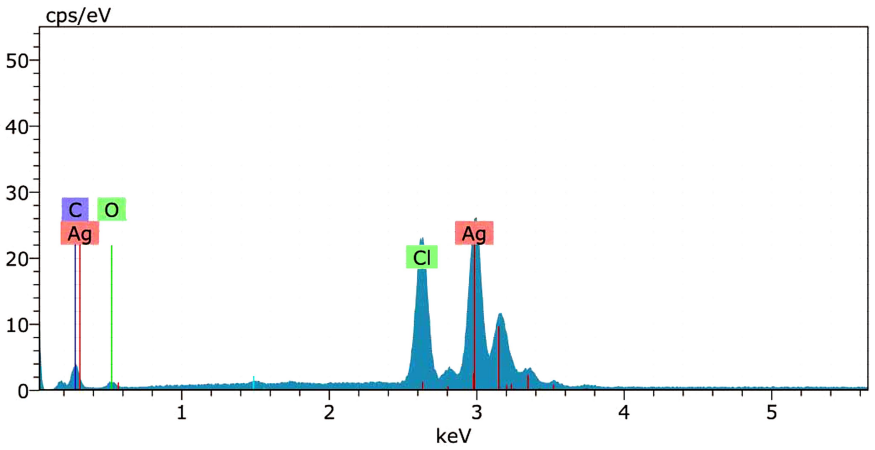

Figure 5 Energy dispersive X-ray (EDX) spectrum analysis of biosynthesized AgNPs using culture supernatant of *Shewanella* sp. ARY1.

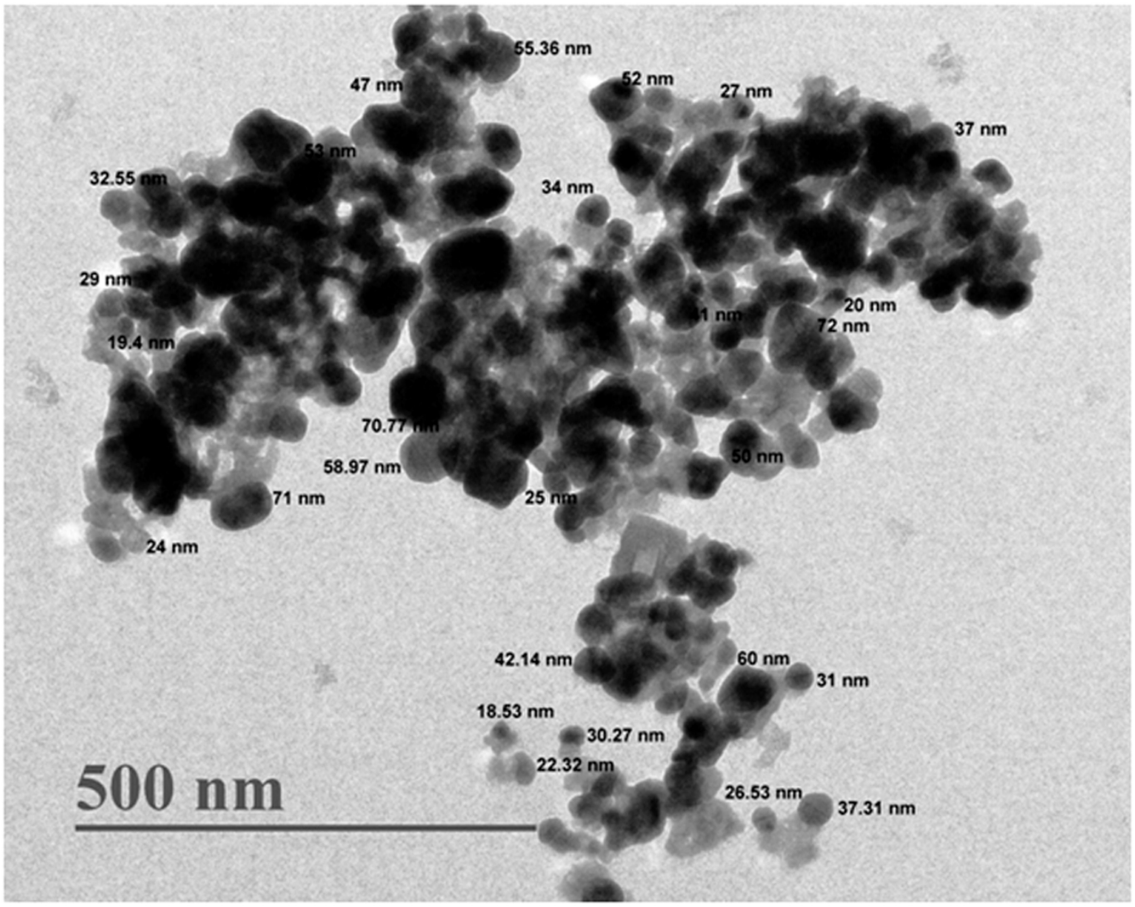

Figure 6 Transmission electron microscopy (TEM) image of biosynthesized AgNPs.

for bacteria to easily develop resistance against AgNPs.[15,20,24,26,27] So, the scientific community shifted their interests on AgNPs, as an alternative strategy, to serve as a potent antibacterial agent. Therefore, in the present study, we have biosynthesized AgNPs using an efficient bacterial strain *Shewanella* sp. ARY1, isolated from the river Yamuna, Delhi. The genus *Shewanella* is well known for its metal reduction ability, and previously, it has been used for the synthesis of various metal nanoparticles, including AgNPs.[38,56] A previous study reported

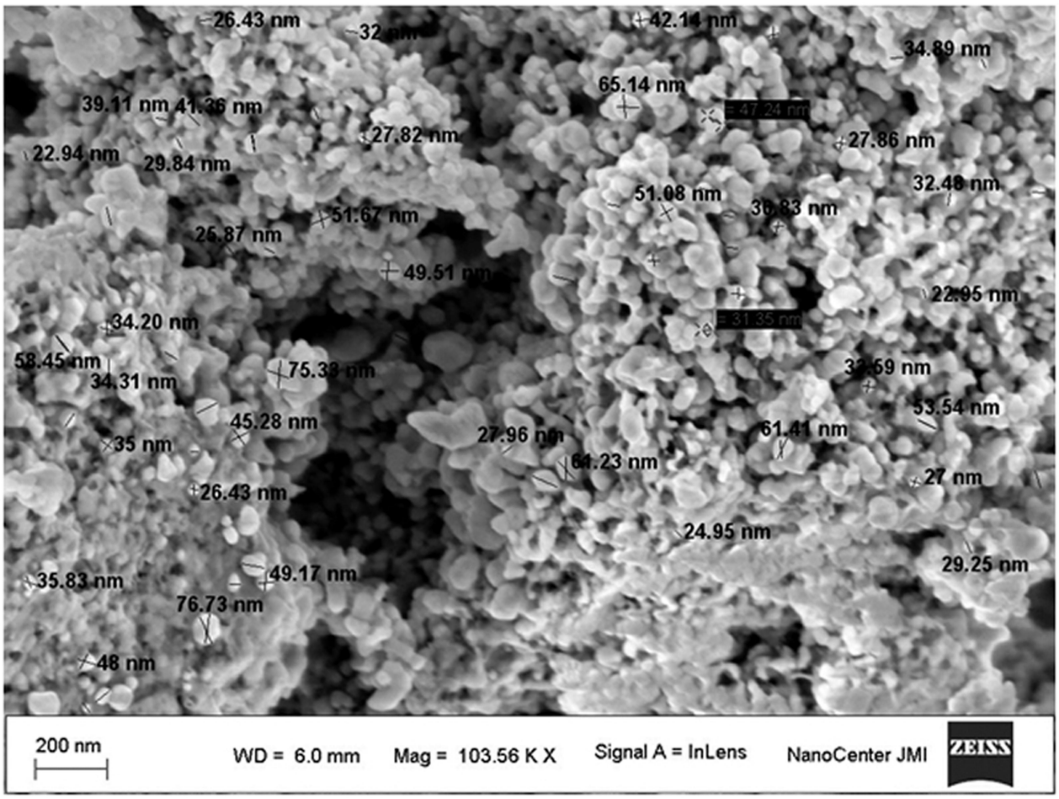

Figure 7 Scanning electron microscopy (SEM) image of biosynthesized AgNPs.

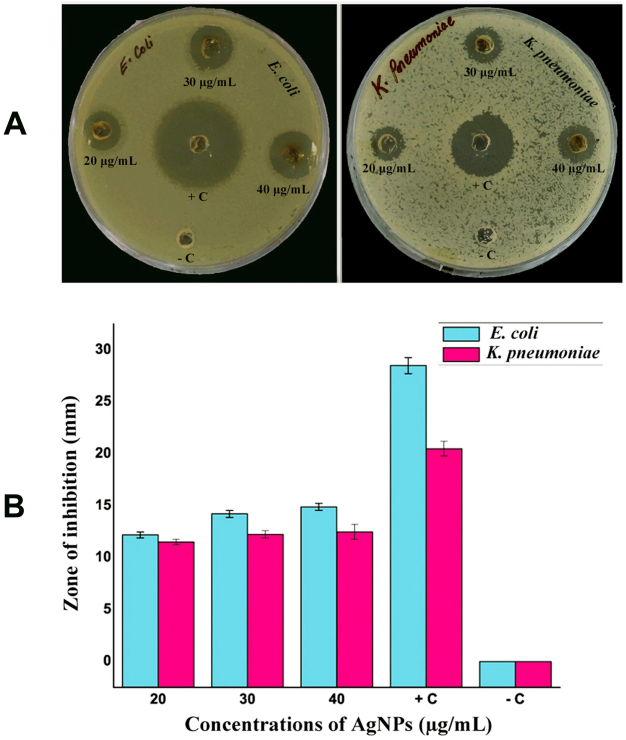

Figure 8 Plates showing clear ZOI around the wells represent the antibacterial activity of biosynthesized AgNPs (**A**), mean diameter (mm) of ZOI for different concentrations of AgNPs against *E. coli* and *K. pneumoniae* (**B**). + C (positive control), antibiotic cefotaxime; - C (negative control), culture supernatant.

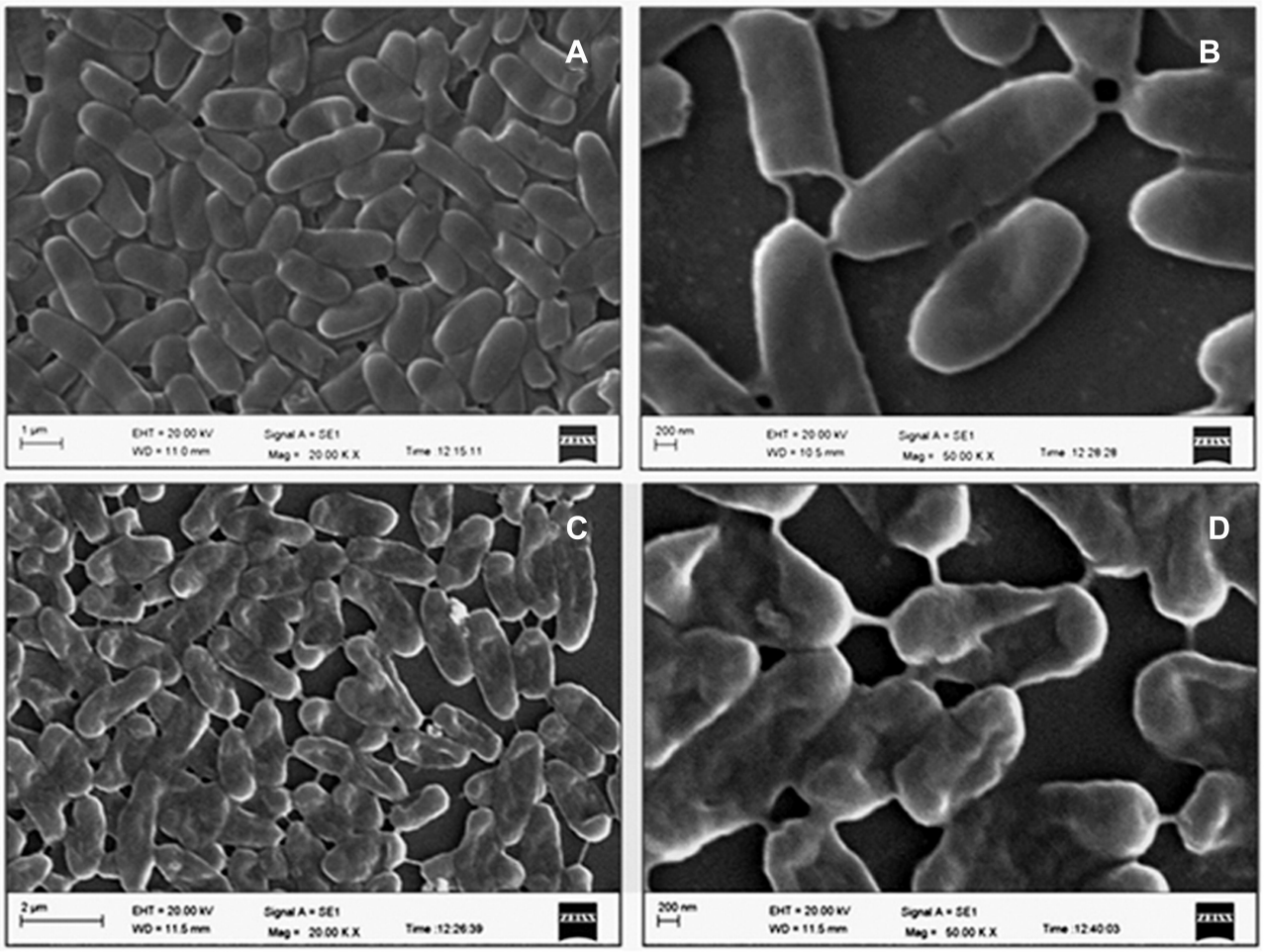

Figure 9 Scanning electron microscopy images of *K. pneumoniae* showing morphological alteration after treatment with biosynthesized AgNPs for 4 h. Untreated control (**A, B**), and cells treated with 32 µg/mL of AgNPs (**C, D**).

the biosynthesis of AgNPs using wild type reference strain *Shewanella oneidensis* MR-1 within 48 h.[38] In the present study, *Shewanella* sp. ARY1 culture supernatant mediated biosynthesis of AgNPs was completed within 6 h, indicating that the process was relatively faster than the previous report.[38] The *Shewanella* genus are also capable of synthesizing others metal nanoparticles like gold, copper, iron and palladium.[41,42,56]

In the present study, biosynthesis of AgNPs occurred when the culture supernatant was mixed with $AgNO_3$ solution at a final concentration of 1 mM and incubated at 35°C. The formation of AgNPs was initially indicated by the appearance of brown color during incubation (Figure 2), which occurs due to surface plasmon resonance (SPR), which is a characteristic feature of AgNPs.[57] Further, UV-Vis spectroscopy analysis showed a strong absorbance peak centered at 450 nm, confirming the synthesis of AgNPs (Figure 2).[10,23,58] Under similar condition, the UV-Vis spectrum analysis of control suspension (LB with 1 mM $AgNO_3$) indicate the synthesis of bigger sizes with different shapes of AgNPs, may be due to aggregations and lack of capping agents (Figure S1). On the other hand, ARY1 culture supernatant exhibited more efficiency for reduction as well as better control over the synthesis of spherical nano-size AgNPs, which may due to the capping of nanoparticles by bacterial metabolites (Figure 2). Our observations are in line with a previous study by Luo et al., 2018, where different culture media was used to determine the effect on the synthesis of AgNPs.[59] They reported that culture media like Nutrient broth (NB) and Mueller-Hinton broth (MHB) reduced the $AgNO_3$ to AgNPs with different particles size but the involvement of bacterial culture metabolites increased the formation of well-characterized AgNPs. The exact mechanism behind the bacterial culture supernatant mediated biosynthesis of AgNPs is poorly understood. However, reports suggest that extracellular biomolecules

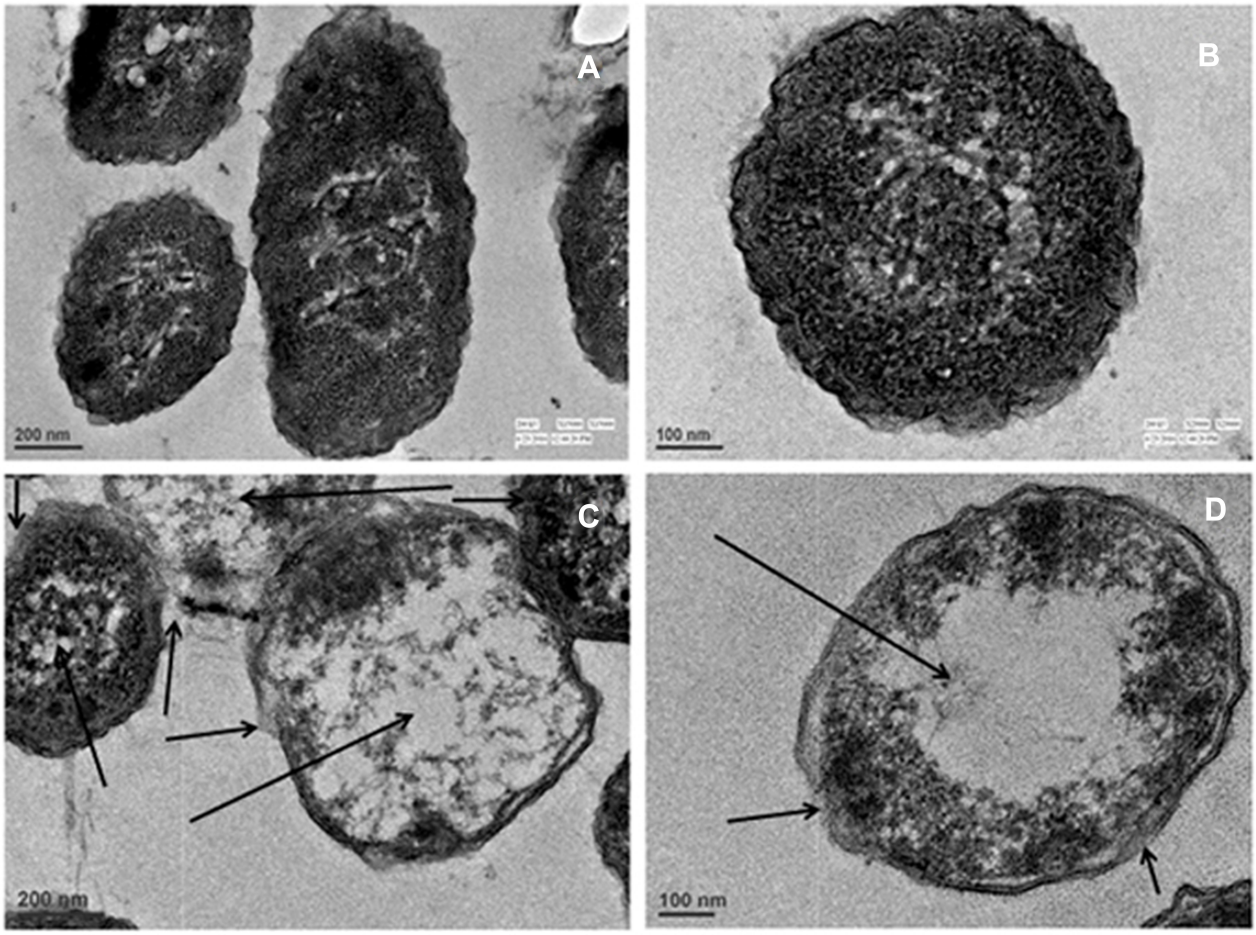

Figure 10 Transmission electron microscopy images of *K. pneumoniae* showing structural alteration after treatment with biosynthesized AgNPs at 32 µg/mL for 4 h (**C, D**), and untreated control (**A, B**). Arrows indicate the cellular damage in *K. pneumoniae* cells treated with AgNPs.

like enzymes, proteins, amino acids, and carbohydrates secreted by bacteria in their culture supernatant play an important role in the reduction of Ag^+ ions to AgNPs and their subsequent stabilization by capping.[37,38,48] Kalimuthu et al., in 2008, reported that bacteria secreted NADPH dependent reductase in the medium that was responsible for the biosynthesis of AgNPs.[40] Therefore, in the present study *Shewanella* sp. ARY1 culture supernatant was used for the biosynthesis of AgNPs.

The FTIR spectrum analysis gives an idea about the possible participation of supernatant biomolecules during the synthesis of AgNPs as the weak peaks observed at 3735 and 3015 cm^{-1} may be due to C-H and O-H stretching vibration of fatty acids and proteins molecules respectively.-[60,61] The strong peaks at 2250 and 1739 cm^{-1} may results from the stretching of C-N and C=O groups, respectively.[62] The peaks at 1627 and 1527 cm^{-1} indicated the presence of N-H group associated with amide I and II of proteins.[47,63,64] The strong bands located at 1368 and 1217 cm^{-1} may arise from the stretching vibration of aromatic amines and ether linkages with AgNPs, respectively.[65,66] A weak peak observed at 1090 cm^{-1} may indicate the bond vibration of the C-O group.[67] Thus, this FTIR data confirmed the association of various active biomolecules with AgNPs during synthesis (Figure 3). Based on FTIR data corroborated with earlier reports, we suggest that *Shewanella* sp. ARY1 supernatant proteins could have possible significant role in the formation as well as capping of AgNPs.[35,68]

The crystalline nature of biosynthesized AgNPs was confirmed by XRD spectrum from four distinct Bragg's reflection peaks (Figure 4). These values are following the reference data of the Joint Committee on Powder Diffraction Standards (JCPDS) file no. 04–0783. In this XRD spectrum, few unassigned peaks were also present, which may arise from supernatant biomolecules capping the AgNPs.[46,69] The above FTIR analysis also confirmed

the association of various biomolecules with AgNPs, which may be responsible for the additional peaks in the XDR spectrum. Previous studies also reported similar kinds of XDR spectrum for extracellular synthesis of AgNPs.[39,46] The XRD data analysis revealed the grain size of AgNPs as 32.97 nm, which was in agreement with the TEM data. Generally, the grain size obtained from XRD data is smaller than the particles size determined by the TEM analysis.[70] Previous studies have also reported smaller crystallite size of the AgNPs than as seen in the TEM analysis.[17,48,71] Further, a strong elemental signal at 3 keV was observed in the EDX spectrum for metallic silver (Figure 5), confirming the successful synthesis of AgNPs.[72] The EDX spectrum also showed some other peaks for Cl, C and O, which may result due to emission from proteins or enzymes present in the bacterial culture supernatant. A similar kind of EDX spectrum has been reported in previous studies for the extracellular synthesis of AgNPs.[73,74] In addition, the presence of Cl peak in the EDX spectrum was possibly due to emissions of bacterial metabolites like proteins, enzymes, carbohydrates, sugars and amino groups.[75,76] These results are in line with other reports of bacteria-mediated biosynthesis of AgNPs.[40,75] The biosynthesized AgNPs were spherical with an average size of 38 nm. The TEM and SEM data observed in this study have a good correlation with previous reports.[36,46] Another study reported AgNPs with an average size of 4±1.5 nm using the *Shewanella oneidensis* MR-1.[38] The variation in product size may be due to the use of bacterial biomass for the synthesis process instead of culture supernatant as used in the current study. Further, different species of *Shewanella* was used in that study, which may have different potential for the biosynthesis of AgNPs with another size.

The potent antibacterial properties of AgNPs against *E. coli* and *K. pneumoniae* were confirmed by the appearance of clear ZOI in the well diffusion assay (Figure 8A). The diameter of ZOI increased with the increasing concentration of AgNPs in the wells. Generally, the size of ZOI is directly related to the susceptibility of the bacterial strain to the test agent, if any strain is sensitive towards any antibacterial agent, exhibits larger ZOI, whereas if the strain is resistant towards the test agent, exhibits smaller ZOI (CLSI-2018).[50] Further, we determined the MIC and MBC of AgNPs against both *E. coli* and *K. pneumoniae*. The MIC values were in the range of 8–16 µg/mL, while MBC was the same i.e., 32 µg/mL for both the tested strains. The antibacterial results have good correlation with previous studies reporting the efficacy of AgNPs against Gram-negative bacteria.[25,77,78] Further, the MBC/MIC ratio, which may reflect the antibacterial spectrum capacity of the tested agent.[79,80] In the present study, the tested strains have tolerance level ≤4 indicating the bactericidal nature of biosynthesized AgNPs. Previously studies have also reported biosynthesized AgNPs as bactericidal agent against Gram-negative bacteria.[21,80] The present results suggested that the biosynthesized AgNPs may be used to treat Gram-negative pathogens. Although AgNPs are well established for their antibacterial properties, their exact mode of action is poorly understood. Therefore, we studied the effect of AgNPs on *K. pneumoniae* by SEM and TEM analysis. The SEM images analysis revealed that AgNPs can damage the outer membrane of Gram-negative bacteria, leading to cell death (Figure 9C and D). Further, TEM images analysis suggested that AgNPs were responsible for damaging the cell structure and release of cytoplasmic contents, leading to cell death (Figure 10C and D). Similar electron microscopy observations regarding the effect of AgNPs on Gram-negative bacteria have been reported earlier as well.[24,26,27]

The toxicity assessment of AgNPs is very essential due to its increasing demand in various biomedical fields for human welfare. The concentration dependent hemolytic activity of AgNPs has also been reported by previous studies.[1,81] According to the American Society for Testing and Materials (ASTM E2524-08) standard guidelines, those materials causing <5% hemolysis are considered as hemocompatible. Our biosynthesized AgNPs showed

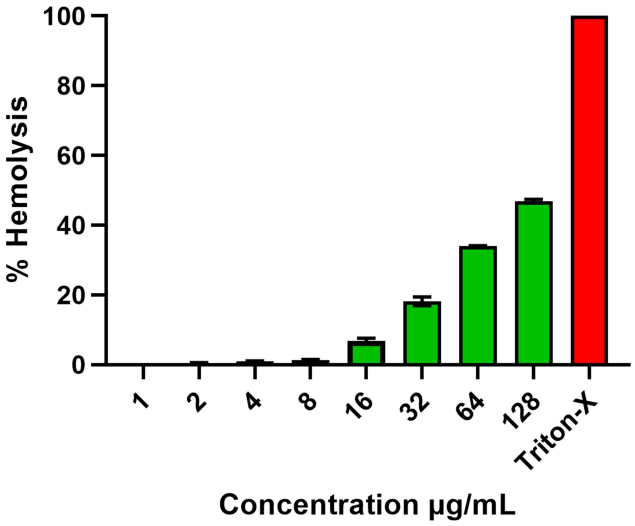

Figure 11 Percentage hemolysis of mice RBCs caused by biosynthesized AgNPs. Triton-X-100 (0.1%) was used as positive control.

hemocompatibility up to the concentration of 8 µg/mL (Figure 11). Hamouda et al., in 2019, also reported low concentrations of biosynthesized AgNPs to be nontoxic to RBC.[1] Thus, the result of the present study indicating the safety of these biosynthesized AgNPs at low concentrations provides support for further investigations.

Conclusion

In the present study, AgNPs were biosynthesized using culture supernatant of *Shewanella* sp. ARY1 via an extracellular approach in an eco-friendly manner to avoid the toxicity of conventional methods. The FTIR analysis revealed the involvement of various supernatant biomolecules, as reducing and capping agents in the synthesis of AgNPs. The biosynthesized AgNPs were crystalline, metallic, and spherical with an average size of 38 nm confirmed by XRD, EDX, TEM, and SEM analysis. The biosynthesis of AgNPs was comparatively faster than the previous reports with the same genus of bacteria might be useful for industrial production. The biosynthesized AgNPs showed effective antibacterial activity against the Gram-negative bacteria *E. coli* and *K. pneumoniae*. Further, electron microscopy analysis of treated cells revealed that AgNPs can damage the outer membrane, subsequent release of cytoplasmic contents, and alter the normal morphology of Gram-negative bacteria, leading to cell death. Encouragingly, the biosynthesized AgNPs were hemocompatible up to the concentration of 8 µg/mL and exhibited low hemolytic activity (6.83±0.75%) up to the concentration of 16 µg/mL, suggesting that they may be used for further antimicrobial study. Thus, the eco-friendly approach established in the present study could be used as an alternative to conventional methods for the synthesis of AgNPs. Further, biosynthesized AgNPs exhibited excellent antibacterial activity, which suggests their potential as candidates to combat Gram-negative pathogens.

Acknowledgments

AHM is grateful to CSIR, India for Research Associateship (File No. 09/263(1185)/2019-EMR-I). SM is grateful to DST-SERB for National Post Doctoral Fellowship (File No. PDF/2017/000549). KM is also grateful for receiving funds from DST-SERB (EMR/2016/001708) and DBT (BT/PR27737/MED/29/1265/2018). Authors acknowledge AIRF, JNU, New Delhi, India for electron microscopy study. We also acknowledge CIF, JMI, New Delhi, India for providing FTIR, SEM with EDX and XRD facilities. We thank Dr. Benu Dhawan, AIIMS, New Delhi, India for kindly providing bacterial ATCC strains.

Disclosure

The authors report no conflicts of interest in this work.

References

1. Hamouda RA, Hussein MH, Abo-Elmagd RA, Bawazir SS. Synthesis and biological characterization of silver nanoparticles derived from the cyanobacterium *Oscillatoria limnetica*. *Sci Rep*. 2019;9(1):13071. doi:10.1038/s41598-019-49444-y
2. Jamkhande PG, Ghule NW, Bamer AH, Kalaskar MG. Metal nanoparticles synthesis: an overview on methods of preparation, advantages and disadvantages, and applications. *J Drug Deliv Sci Technol*. 2019;53:101174. doi:10.1016/j.jddst.2019.101174
3. Kulkarni N, Muddapur U. Biosynthesis of metal nanoparticles: a review. *J Nanotechnol*. 2014;2014:510246. doi:10.1155/2014/510246
4. Li X, Robinson SM, Gupta A, et al. Functional gold nanoparticles as potent antimicrobial agents against multi-drug-resistant bacteria. *ACS Nano*. 2014;8(10):10682–10686. doi:10.1021/nn5042625
5. Salem SS, Fouda A. Green synthesis of metallic nanoparticles and their prospective biotechnological applications: an overview. *Biol Trace Elem Res*. 2020;1–27.
6. Hassan SE, Fouda A, Radwan AA, et al. Endophytic actinomycetes *Streptomyces* spp mediated biosynthesis of copper oxide nanoparticles as a promising tool for biotechnological applications. *J Biol Inorg Chem*. 2019;24(3):377–393. doi:10.1007/s00775-019-01654-5
7. Mohamed AA, Fouda A, Abdel-Rahman MA, et al. Fungal strain impacts the shape, bioactivity and multifunctional properties of green synthesized zinc oxide nanoparticles. *Biocatal Agric Biotechnol*. 2019;19:101103. doi:10.1016/j.bcab.2019.101103
8. Fouda A, El-Din Hassan S, Salem SS, Shaheen TI. *In-Vitro* cytotoxicity, antibacterial, and UV protection properties of the biosynthesized Zinc oxide nanoparticles for medical textile applications. *Microb Pathog*. 2018;125:252–261. doi:10.1016/j.micpath.2018.09.030
9. Hassan SELD, Salem SS, Fouda A, Awad MA, El-Gamal MS, Abdo AM. New approach for antimicrobial activity and bio-control of various pathogens by biosynthesized copper nanoparticles using endophytic actinomycetes. *J Radiat Res Appl Sci*. 2018;11(3):262–270. doi:10.1016/j.jrras.2018.05.003
10. Fouda A, Hassan SE, Abdo AM, El-Gamal MS. Antimicrobial, antioxidant and larvicidal activities of spherical silver nanoparticles synthesized by endophytic *Streptomyces* spp. *Biol Trace Elem Res*. 2020;195(2):707–724. doi:10.1007/s12011-019-01883-4
11. Fouda A, Abdel-Maksoud G, Abdel-Rahman MA, Salem SS, Hassan SE-D, El-Sadany MA-H. Eco-friendly approach utilizing green synthesized nanoparticles for paper conservation against microbes involved in biodeterioration of archaeological manuscript. *Int Biodeterior Biodegradation*. 2019;142:160–169. doi:10.1016/j.ibiod.2019.05.012
12. Fouda A, Abdel-Maksoud G, Abdel-Rahman MA, Eid AM, Barghoth MG, El-Sadany MA-H. Monitoring the effect of biosynthesized nanoparticles against biodeterioration of cellulose-based materials by *Aspergillus niger*. *Cellulose*. 2019;26(11):6583–6597. doi:10.1007/s10570-019-02574-y
13. Cheon JY, Kim SJ, Rhee YH, Kwon OH, Park WH. Shape-dependent antimicrobial activities of silver nanoparticles. *Int J Nanomedicine*. 2019;14:2773–2780. doi:10.2147/IJN.S196472
14. Burdușel AC, Gherasim O, Grumezescu AM, Mogoantă L, Ficai A, Andronescu E. Biomedical applications of silver nanoparticles: an up-to-date overview. *Nanomaterials (Basel)*. 2018;8:9.
15. Siddiqi KS, Husen A, Rao RAK. A review on biosynthesis of silver nanoparticles and their biocidal properties. *J Nanobiotechnology*. 2018;16(1):14.
16. Kedi PBE, Meva FE, Kotsedi L, et al. Eco-friendly synthesis, characterization, in vitro and in vivo anti-inflammatory activity of silver nanoparticle-mediated *Selaginella myosurus* aqueous extract. *Int J Nanomedicine*. 2018;13:8537–8548. doi:10.2147/IJN.S174530

17. El-Naggar NE, Hussein MH, El-Sawah AA. Bio-fabrication of silver nanoparticles by phycocyanin, characterization, *in vitro* anticancer activity against breast cancer cell line and *in vivo* cytotoxicity. *Sci Rep*. 2017;7(1):10844.
18. Rafique M, Sadaf I, Rafique MS, Tahir MB. A review on green synthesis of silver nanoparticles and their applications. *Artif Cells Nanomed Biotechnol*. 2017;45(7):1272–1291. doi:10.1080/21691401.2016.1241792
19. Ghodake G, Kim M, Sung JS, et al. Extracellular synthesis and characterization of silver nanoparticles-antibacterial activity against multidrug-resistant bacterial strains. *Nanomaterials (Basel)*. 2020;10:2. doi:10.3390/nano10020360
20. Le Ouay B, Stellacci F. Antibacterial activity of silver nanoparticles: a surface science insight. *Nano Today*. 2015;10(3):339–354. doi:10.1016/j.nantod.2015.04.002
21. Mohammed AE, Al-Qahtani A, Al-Mutairi A, Al-Shamri B, Aabed KF. Antibacterial and cytotoxic potential of biosynthesized silver nanoparticles by some plant extracts. *Nanomaterials (Basel)*. 2018;8:6. doi:10.3390/nano8060382
22. Behravan M, Hossein Panahi A, Naghizadeh A, Ziaee M, Mahdavi R, Mirzapour A. Facile green synthesis of silver nanoparticles using *Berberis vulgaris* leaf and root aqueous extract and its antibacterial activity. *Int J Biol Macromol*. 2019;124:148–154. doi:10.1016/j.ijbiomac.2018.11.101
23. Pirtarighat S, Ghannadnia M, Baghshahi S. Green synthesis of silver nanoparticles using the plant extract of *Salvia spinosa* grown *in vitro* and their antibacterial activity assessment. *J Nanostructure Chem*. 2019;9(1):1–9. doi:10.1007/s40097-018-0291-4
24. Liao S, Zhang Y, Pan X, et al. Antibacterial activity and mechanism of silver nanoparticles against multidrug-resistant *Pseudomonas aeruginosa*. *Int J Nanomedicine*. 2019;14:1469–1487. doi:10.2147/IJN.S191340
25. Mondal AH, Yadav D, Ali A, Khan N, Jin JO, Haq QMR. Antibacterial and anti-candidal activity of silver nanoparticles biosynthesized using *Citrobacter* spp. MS5 culture supernatant. *Biomolecules*. 2020;10(6):944. doi:10.3390/biom10060944
26. Ontong JC, Paosen S, Shankar S, Voravuthikunchai SP. Eco-friendly synthesis of silver nanoparticles using *Senna alata* bark extract and its antimicrobial mechanism through enhancement of bacterial membrane degradation. *J Microbiol Methods*. 2019;165:105692. doi:10.1016/j.mimet.2019.105692
27. Marslin G, Selvakesavan RK, Franklin G, Sarmento B, Dias AC. Antimicrobial activity of cream incorporated with silver nanoparticles biosynthesized from Withania somnifera. *Int J Nanomedicine*. 2015;10:5955–5963.
28. Guilger M, Pasquoto-Stigliani T, Bilesky-Jose N, et al. Biogenic silver nanoparticles based on *trichoderma harzianum*: synthesis, characterization, toxicity evaluation and biological activity. *Sci Rep*. 2017;7:44421. doi:10.1038/srep44421
29. Iravani S, Korbekandi H, Mirmohammadi SV, Zolfaghari B. Synthesis of silver nanoparticles: chemical, physical and biological methods. *Res Pharm Sci*. 2014;9(6):385–406.
30. Ahmad S, Munir S, Zeb N, et al. Green nanotechnology: a review on green synthesis of silver nanoparticles - an ecofriendly approach. *Int J Nanomedicine*. 2019;14:5087–5107. doi:10.2147/IJN.S200254
31. Huq MA. Green synthesis of silver nanoparticles using *Pseudoduganella eburnea* MAHUQ-39 and their antimicrobial mechanisms investigation against drug resistant human pathogens. *Int J Mol Sci*. 2020;21:4. doi:10.3390/ijms21041510
32. Gahlawat G, Choudhury AR. A review on the biosynthesis of metal and metal salt nanoparticles by microbes. *RSC Adv*. 2019;9(23):12944–12967. doi:10.1039/C8RA10483B
33. Vaidyanathan R, Gopalram S, Kalishwaralal K, Deepak V, Pandian SR, Gurunathan S. Enhanced silver nanoparticle synthesis by optimization of nitrate reductase activity. *Colloids Surf B Biointerfaces*. 2010;75(1):335–341. doi:10.1016/j.colsurfb.2009.09.006
34. Ganesh Babu MM, Gunasekaran P. Production and structural characterization of crystalline silver nanoparticles from *Bacillus cereus* isolate. *Colloids Surf B Biointerfaces*. 2009;74(1):191–195. doi:10.1016/j.colsurfb.2009.07.016
35. Priyadarshini S, Gopinath V, Meera Priyadharsshini N, MubarakAli D, Velusamy P. Synthesis of anisotropic silver nanoparticles using novel strain, *Bacillus flexus* and its biomedical application. *Colloids Surf B Biointerfaces*. 2013;102:232–237. doi:10.1016/j.colsurfb.2012.08.018
36. Shanthi S, Jayaseelan BD, Velusamy P, Vijayakumar S, Chih CT, Vaseeharan B. Biosynthesis of silver nanoparticles using a probiotic *Bacillus licheniformis* Dahb1 and their antibiofilm activity and toxicity effects in Ceriodaphnia cornuta. *Microb Pathog*. 2016;93:70–77. doi:10.1016/j.micpath.2016.01.014
37. Singh H, Du J, Singh P, Yi TH. Extracellular synthesis of silver nanoparticles by *Pseudomonas* sp. THG-LS1.4 and their antimicrobial application. *J Pharm Anal*. 2018;8(4):258–264.
38. Suresh AK, Pelletier DA, Wang W, et al. Silver nanocrystallites: biofabrication using *Shewanella oneidensis*, and an evaluation of their comparative toxicity on Gram-negative and Gram-positive bacteria. *Environ Sci Technol*. 2010;44(13):5210–5215. doi:10.1021/es903684r
39. Malarkodi C, Rajeshkumar S, Paulkumar K, Vanaja M, Jobitha GDG, Annadurai G. Bactericidal activity of bio mediated silver nanoparticles synthesized by *Serratia nematodiphila*. *Drug Invention Today*. 2013;5(2):119–125.
40. Kalimuthu K, Suresh Babu R, Venkataraman D, Bilal M, Gurunathan S. Biosynthesis of silver nanocrystals by *Bacillus licheniformis*. *Colloids Surf B Biointerfaces*. 2008;65(1):150–153. doi:10.1016/j.colsurfb.2008.02.018
41. Huang BC, Yi YC, Chang JS, Ng IS. Mechanism study of photo-induced gold nanoparticles formation by *Shewanella oneidensis* MR-1. *Sci Rep*. 2019;9(1):7589. doi:10.1038/s41598-019-44088-4
42. Kimber RL, Lewis EA, Parmeggiani F, et al. Biosynthesis and characterization of copper nanoparticles using *Shewanella oneidensis*: application for click chemistry. *Small*. 2018;14:10. doi:10.1002/smll.201703145
43. Kaye KS, Pogue JM. Infections caused by resistant Gram-negative bacteria: epidemiology and management. *Pharmacotherapy*. 2015;35(10):949–962.
44. Doi Y, Bonomo RA, Hooper DC, et al. Gram-negative bacterial infections: research priorities, accomplishments, and future directions of the antibacterial resistance leadership group. *Clin Infect Dis*. 2017;64(suppl 1):S30–S35. doi:10.1093/cid/ciw829
45. Gopinath V, Priyadarshini S, Loke MF, et al. Biogenic synthesis, characterization of antibacterial silver nanoparticles and its cell cytotoxicity. *Arabian J Chemistry*. 2017;10(8):1107–1117. doi:10.1016/j.arabjc.2015.11.011
46. Kalpana D, Lee YS. Synthesis and characterization of bactericidal silver nanoparticles using cultural filtrate of simulated microgravity grown *Klebsiella pneumoniae*. *Enzyme Microb Technol*. 2013;52(3):151–156. doi:10.1016/j.enzmictec.2012.12.006
47. Costa Silva LP, Oliveira JP, Keijok WJ, et al. Extracellular biosynthesis of silver nanoparticles using the cell-free filtrate of nematophagous fungus *Duddingtonia flagrans*. *Int J Nanomedicine*. 2017;12:6373–6381. doi:10.2147/IJN.S137703
48. Hamida RS, Abdelmeguid NE, Ali MA, Bin-Meferij MM, Khalil MI. Synthesis of silver nanoparticles using a novel cyanobacteria *Desertifilum* sp. extract: their antibacterial and cytotoxicity effects. *Int J Nanomedicine*. 2020;15:49–63.
49. Jalal M, Ansari MA, Alzohairy MA, et al. Biosynthesis of silver nanoparticles from oropharyngeal *Candida glabrata isolates and their antimicrobial activity against clinical strains of bacteria*and fungi. *Nanomaterials (Basel)*. 2018;8:8. doi:10.3390/nano8080586
50. Wayne PA. *Performance Standards for Antimicrobial Susceptibility Testing* (supplement M100) 28th ed. Clinical and Laboratory Standards Institute CLSI;2018.

51. May J, Shannon K, King A, French G. Glycopeptide tolerance in *Staphylococcus aureus*. *J Antimicrob Chemother*. 1998;42(2):189–197. doi:10.1093/jac/42.2.189
52. Kumar P, Kandi SK, Manohar S, Mukhopadhyay K, Rawat DS. Monocarbonyl curcuminoids with improved stability as antibacterial agents against *Staphylococcus aureus* and their mechanistic studies. *ACS Omega*. 2019;4(1):675–687. doi:10.1021/acsomega.8b02625
53. Singh M, Mukhopadhyay K. C-terminal amino acids of alpha-melanocyte-stimulating hormone are requisite for its antibacterial activity against *Staphylococcus aureus*. *Antimicrob Agents Chemother*. 2011;55(5):1920–1929. doi:10.1128/AAC.00957-10
54. Mohammed AE. Green synthesis, antimicrobial and cytotoxic effects of silver nanoparticles mediated by *Eucalyptus camaldulensis* leaf extract. *Asian Pac J Trop Biomed*. 2015;5(5):382–386. doi:10.1016/S2221-1691(15)30373-7
55. Siddiqui MT, Mondal AH, Sultan I, Ali A, Haq QMR. Co-occurrence of ESBLs and silver resistance determinants among bacterial isolates inhabiting polluted stretch of river Yamuna, India. *Int J Environ Sci Technol*. 2019;16(10):5611–5622. doi:10.1007/s13762-018-1939-9
56. Kim TY, Kim MG, Lee JH, Hur HG. Biosynthesis of nanomaterials by *Shewanella* species for application in lithium ion batteries. *Front Microbiol*. 2018;9:2817. doi:10.3389/fmicb.2018.02817
57. Mohammed AE, Bin Baz FF, Albrahim JS. *Calligonum comosum* and *Fusarium* sp. extracts as bio-mediator in silver nanoparticles formation: characterization, antioxidant and antibacterial capability. *3 Biotech*. 2018;8(1):72.
58. Das VL, Thomas R, Varghese RT, Soniya EV, Mathew J, Radhakrishnan EK. Extracellular synthesis of silver nanoparticles by the *Bacillus* strain CS 11 isolated from industrialized area. *3 Biotech*. 2014;4(2):121–126. doi:10.1007/s13205-013-0130-8
59. Luo K, Jung S, Park K-H, Kim Y-R. Microbial biosynthesis of silver nanoparticles in different culture media. *J Agric Food Chem*. 2018;66(4):957–962. doi:10.1021/acs.jafc.7b05092
60. Gopinath PM, Ranjani A, Dhanasekaran D, et al. Multi-functional nano silver: a novel disruptive and theranostic agent for pathogenic organisms in real-time. *Sci Rep*. 2016;6:34058. doi:10.1038/srep34058
61. Faghihzadeh F, Anaya NM, Schifman LA, Oyanedel-Craver V. Fourier transform infrared spectroscopy to assess molecular-level changes in microorganisms exposed to nanoparticles. *Nanotechnol Environ Eng*. 2016;1(1):1.
62. Jena J, Pradhan N, Nayak RR, et al. Microalga Scenedesmus sp.: a potential low-cost green machine for silver nanoparticle synthesis. *J Microbiol Biotechnol*. 2014;24(4):522–533.
63. Gajbhiye M, Kesharwani J, Ingle A, Gade A, Rai M. Fungus-mediated synthesis of silver nanoparticles and their activity against pathogenic fungi in combination with fluconazole. *Nanomedicine*. 2009;5(4):382–386. doi:10.1016/j.nano.2009.06.005
64. Syed A, Saraswati S, Kundu GC, Ahmad A. Biological synthesis of silver nanoparticles using the fungus *Humicola* sp. and evaluation of their cytotoxicity using normal and cancer cell lines. *Spectrochim Acta A Mol Biomol Spectrosc*. 2013;114:144–147. doi:10.1016/j.saa.2013.05.030
65. Thomas R, Nair AP, Kr S, Mathew J, Ek R. Antibacterial activity and synergistic effect of biosynthesized AgNPs with antibiotics against multidrug-resistant biofilm-forming coagulase-negative Staphylococci isolated from clinical samples. *Appl Biochem Biotechnol*. 2014;173(2):449–460. doi:10.1007/s12010-014-0852-z
66. Malapermal V, Botha I, Krishna SBN, Mbatha JN. Enhancing antidiabetic and antimicrobial performance of *Ocimum basilicum*, and *Ocimum sanctum* (L.) using silver nanoparticles. *Saudi J Biol Sci*. 2017;24(6):1294–1305. doi:10.1016/j.sjbs.2015.06.026
67. Sathishkumar RS, Sundaramanickam A, Srinath R, et al. Green synthesis of silver nanoparticles by bloom forming marine microalgae *Trichodesmium erythraeum* and its applications in antioxidant, drug-resistant bacteria, and cytotoxicity activity. *J Saudi Chem Soc*. 2019;23(8):1180–1191.
68. Fayaz AM, Balaji K, Girilal M, Yadav R, Kalaichelvan PT, Venketesan R. Biogenic synthesis of silver nanoparticles and their synergistic effect with antibiotics: a study against gram-positive and gram-negative bacteria. *Nanomedicine*. 2010;6(1):103–109.
69. Kalishwaralal K, Deepak V, Ram Kumar Pandian S, et al. Biosynthesis of silver and gold nanoparticles using *Brevibacterium casei*. *Colloids Surf B Biointerfaces*. 2010;77(2):257–262.
70. Ungár T, Tichy G, Gubicza J, Hellmig RJ. Correlation between subgrains and coherently scattering domains. *Powder Diffraction*. 2005;20(4):366–375.
71. Sarli S, Kalani MR, Moradi A. A potent and safer anticancer and antibacterial taxus-based green synthesized silver nanoparticle. *Int J Nanomedicine*. 2020;15:3791–3801. doi:10.2147/IJN.S251174
72. Park J, Joo J, Kwon SG, Jang Y, Hyeon T. Synthesis of monodisperse spherical nanocrystals. *Angew Chem Int Ed Engl*. 2007;46(25):4630–4660.
73. Jyoti K, Baunthiyal M, Singh A. Characterization of silver nanoparticles synthesized using *Urtica dioica* Linn. Leaves and their synergistic effects with antibiotics. *J Radiat Res Appl Sci*. 2016;9(3):217–227.
74. Kumar CG, Mamidyala SK. Extracellular synthesis of silver nanoparticles using culture supernatant of *Pseudomonas aeruginosa*. *Colloids Surf B Biointerfaces*. 2011;84(2):462–466.
75. Alsharif SM, Salem SS, Abdel-Rahman MA, et al. Multifunctional properties of spherical silver nanoparticles fabricated by different microbial taxa. *Heliyon*. 2020;6(5):e03943. doi:10.1016/j.heliyon.2020.e03943
76. Manivasagan P, Venkatesan J, Senthilkumar K, Sivakumar K, Kim S-K. Biosynthesis, antimicrobial and cytotoxic effect of silver nanoparticles using a novel *Nocardiopsis* sp. MBRC-1. *BioMed Res Int*. 2013;2013:287638.
77. Shu M, He F, Li Z, et al. Biosynthesis and antibacterial activity of silver nanoparticles using yeast extract as reducing and capping agents. *Nanoscale Res Lett*. 2020;15(1):14. doi:10.1186/s11671-019-3244-z
78. Guzman M, Dille J, Godet S. Synthesis and antibacterial activity of silver nanoparticles against gram-positive and gram-negative bacteria. *Nanomedicine*. 2012;8(1):37–45.
79. Woods GL, Washington JA. The clinician and the microbiology laboratory. In: Mandell G, Bennett J, Dolin R, editors. *Principles and Practice of Infectious Diseases*. 4th ed. Philadelphia (NY): Churchill Livingstone; 1995;169–199.
80. Das B, Dash SK, Mandal D, et al. Green synthesized silver nanoparticles destroy multidrug resistant bacteria via reactive oxygen species mediated membrane damage. *Arabian J Chem*. 2017;10(6):862–876. doi:10.1016/j.arabjc.2015.08.008
81. Parthiban E, Manivannan N, Ramanibai R, Mathivanan N. Green synthesis of silver-nanoparticles from *Annona reticulata* leaves aqueous extract and its mosquito larvicidal and anti-microbial activity on human pathogens. *Biotechnol Rep (Amst)*. 2019;21:e00297.